Received: 11 April 2021 | Revised: 14 June 2021 | Accepted: 21 June 2021

DOI: 10.1111/iwj.13653

ORIGINAL ARTICLE

IWJ WILEY

The influence of a biofilm-dispersing wound gel on the wound healing process

Kayla Bounds[1,2] | **Jane A. Colmer-Hamood**[2,3] | **Matthew Myntti**[4] | **Randall M. Jeter**[1] | **Abdul N. Hamood**[2,5]

[1]Department of Biological Sciences, Texas Tech University, Lubbock, Texas, USA

[2]Department of Immunology and Molecular Microbiology, Texas Tech University Health Sciences Center, Lubbock, Texas, USA

[3]Department of Medical Education, Texas Tech University Health Sciences Center, Lubbock, Texas, USA

[4]Research and Development, Next Science LLC, Jacksonville, Florida, USA

[5]Department of Surgery, Texas Tech University Health Sciences Center, Lubbock, Texas, USA

Correspondence
Abdul N. Hamood, PhD, Department of Immunology and Molecular Microbiology, Texas Tech University Health Sciences Center, 3601 4th Street STOP 6591, Lubbock, TX 79430–6591, USA.
Email: abdul.hamood@ttuhsc.edu

Funding information
Next Science, LLC; Jacksonville, Florida, USA

Abstract

Topical antimicrobials that reduce the bacterial bioburden within a chronically-infected wound may have helpful or harmful effects on the healing process. We used murine models of full-thickness skin wounds to determine the effects of the novel biofilm-dispersing wound gel (BDWG) and its gel base on the healing of uninfected wounds. The rate of wound closure over 19 days was comparable among the BDWG-treated (BT) wounds and the controls. Compared with the controls, histology of the BT wounds showed formation of a stable blood clot at day 1, more neovascularisation and reepithelialisation at day 3, and more organised healing at day 7. Fluorescence-activated cell sorting analysis showed a lower percentage of neutrophils in wounded tissues of the BT group at days 1 and 3, and significantly more M2 macrophages at day 3. Levels of proinflammatory cytokines and chemokines were increased over the uninjured baseline within the wounds of all treatment groups but the levels were significantly lower in the BT group at day 1, modulating the inflammatory response. Our results suggest that BDWG does not interfere with the wound healing process and may enhance it by lowering inflammation and allowing transition to the proliferative stage of wound healing by day 3.

KEYWORDS

cellular infiltration, cytokines, novel wound therapy, wound closure, wound healing

Key Messages

- the goal of the study was to assess the effect of a novel broad-spectrum antimicrobial agent on the wound healing process
- the study included examining: wound closure rate, histopathological changes within the wounded tissues, immune cell infiltration, and the production of wound related cytokines
- results showed that application of the formulated agent did not interfere with the wound closure rate or any of the four stages of the wound healing process

1 | INTRODUCTION

Wound healing is a very complex process that is characterised by four specific overlapping stages: haemostasis, inflammation, proliferation, and remodelling (Figure 1).[1,2] Within 30 minutes post-wounding, the process of haemostasis leads to formation of a stable fibrin clot that provides a provisional matrix for incoming immune cells (Figure 1).[1,3,4] The inflammatory stage is initiated when plates within the fibrin clot, plus endogenous cell molecules and cytokines and chemokines (C/C) released by injured cells within the wounded tissue recruit neutrophils and M1 macrophages to remove foreign bodies, dead and damaged cells, and bacteria (Figure 1).[5-10] These cells, together with resident immune cells in the skin, secrete a variety of proinflammatory C/C such as IL-6, IL-1β, CCL3, CXCL1, tumor necrosis factor-α, and granulocyte-monocyte colony-stimulating factor (GM-CSF) that recruit additional neutrophils and macrophages to the site of the injury.[5-9] Under the influence of GM-CSF, tissue-dwelling macrophages and recruited monocytes switch to M1 macrophages.[7,8,10,11]

Depending on the size of the wound, neutrophil infiltration slows after 2 to 3 days and the infiltrating neutrophils are triggered to undergo apoptosis by M1 macrophages, which then phagocytose them (efferocytosis).[7,8,10] With the initiation of the proliferation stage in an uninfected wound, macrophages secrete IL-10, vascular endothelial growth factor (VEGF), and other C/C that induce infiltration of the wounded tissue by fibroblasts and vascular endothelial cells (Figure 1).[5,7,8] The proliferation stage is characterised by maturation of the scab over the wound, epidermal hyperplasia at the margins, reepithelialisation, angiogenesis (neovascularisation), and the formation of granulation tissue within the wound.[2,8,12] Additionally, efferocytosis triggers a phenotypic switch of the M1 macrophages to the M2 "anti-inflammatory" phenotype, which are necessary for remodelling of the matrix and final resolution of the wound healing process.[8,11,13]

In the remodelling stage, M2 macrophages secrete IL-10, transforming growth factor-β, and vascular endothelial growth factor (VEGF) promoting replacement of granulation tissue with cellular matrix, continued cell proliferation, synthesis of new extracellular matrix molecules, and angiogenesis (Figure 1).[7,11,13-15] The remodelling stage overlaps the proliferative stage as the wound heals from the margins inward across the bed of the wound. At this stage, the levels of neutrophils within the margin and bed of the wound drop, muscle and fatty tissue regenerate at the margins and granulation tissue forms closer to the centre of the wound; neovascularisation continues while epidermal hyperplasia expands coverage of the wound surface, and hair follicle regeneration occurs (Figure 1).[16,17]

Development of infection within a skin wound is a major hindrance to healing as infected wounds fail to proceed through the stages of healing in a timely manner, becoming chronic wounds that are much more difficult to treat.[18-21] An effective topical treatment for chronic wounds would prevent infection or reduce the wound bioburden significantly while enhancing, or at least not interfering with, the wound healing process by altering the cellular and/or molecular mechanisms of wound healing. We have recently described a novel biofilm dispersal agent (Next Science, Jacksonville, Florida) as a treatment for chronic wounds.[22] Using the murine model of wound infections, we showed that the agent formulated as a wound gel (biofilm-dispersing wound gel—BDWG) prevented and eliminated the growth and proliferation of different gram-positive and gram-negative wound pathogens.[22] However, the effects of BDWG on the wound healing process remain unknown. In this study, we used murine models of full-thickness skin wounds to examine the potential effects of BDWG on different aspects of wound healing in uninfected wounds.

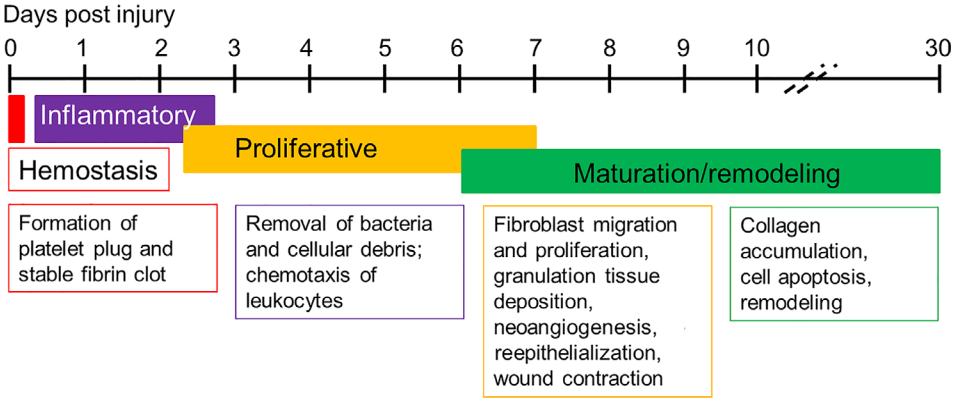

FIGURE 1 Timeline for stages of healing of an uninfected wound in the murine model

2 | MATERIALS AND METHODS

See Table S1 for detailed descriptions and sources of all materials, antibodies, and reagents.

2.1 | Full-thickness skin wound models

Adult female Swiss Webster mice (Charles Rivers Laboratory, Wilmington, Massachusetts) weighing 22 to 25 g were used in the experiments. All animal experiments were carried out in strict accordance with the recommendations in the Guide for the Care and Use of Laboratory Animals of the National Institutes of Health under a protocol approved by the Institutional Animal Care and Use Committee of Texas Tech University Health Sciences Center (TTUHSC).

For most experiments, full-thickness excisional wounds were generated on the backs of mice as previously described.[22,23] Mice were anaesthetised by intraperitoneal injection of 5% sodium pentobarbital at 5 mg/mL, their backs were shaved, disinfected with 70% ethanol, and 1.5 × 1.5 cm full-thickness excisions were made in the skin with surgical scissors, removing the skin and subcutaneous tissues down to the fascia. For analysis of C/C, punch biopsy was used to create the full-thickness wounds as previously described.[24] Mice were prepared as for the excisional model and three full-thickness skin wounds spaced about a cm apart were made on the back of each mouse using 6-mm disposable biopsy punches.

For both models, injured mice were divided into three groups. Wounds of the untreated control (UT) group were covered with a 22 × 22 mm piece of sterile gauze that was secured using a transparent, moisture permeable, adhesive dressing. For the second group of mice, the gauze was spread with 400 mg of water-soluble polyethylene glycol (PEG) gel base (PEG-treated; PT),[22] which consists of PEG 400 plus PEG 3350 that has been shown to be inert, non-pyrogenic, and non-toxic.[25,26] For the third group, the gauze was spread with 400 mg BDWG prior to application to the wound (BDWG-treated; BT).[22] The BDWG consists of PEG gel base containing a proprietary, non-toxic formulation (Xbio™ Technology, Next Science) that disrupts the exopolysaccharide matrix of biofilms found in chronic wounds. This renders the bacteria within the biofilm more susceptible to the antimicrobial effect of the active ingredient benzalkonium chloride, which is incorporated in BDWG at a concentration of 0.13%. Adhesive dressings were then applied over the gauze dressings on all the wounds.

Mice were monitored daily for up to 19 days post-injury/treatment (dPIT) for signs of illness or wound infection (purulent wound exudate, redness of surrounding skin) according to the protocol. At 1, 3, and 7 dPIT, three mice from each group with excisional wounds were euthanised and the wound bed plus approximately 3 mm of intact tissue surrounding the excision wound was excised for further analysis. In the punch biopsy model, an 8-mm biopsy punch was used to collect the wound and margins.

2.2 | Wound closure measurement

Images of the excisional wounds on the backs of three mice in each treatment group were taken at day 0 prior to covering the wounds for the first time. At 1, 3, 7, 10, 13, 16, and 19 dPIT, mice were anaesthetised, the dressings were removed, wound images were taken with a Silhouette wound imaging system (Aranz Medical, Christchurch, New Zealand), and the surface area of each wound was traced. After imaging, a fresh dressing was applied to the wound. The same mice were observed throughout this experiment.

2.3 | Histological examination

Histological analysis was performed on samples obtained from the excisional model. At 1, 3, and 7 dPIT, three mice from each group were euthanised and the wound bed and surrounding intact tissue (about 3 mm) were excised and fixed in 10% formalin. The samples were submitted to the Department of Pathology, TTUHSC, for paraffin embedding and sectioning. Representative paraffin-embedded sections were stained with haematoxylin and eosin (H&E) according to standard protocol[27] and stained sections were coverslipped using Permount mounting medium. Histology of the sections was visualised under 100× and 200× magnification using a Zeiss Axiovert 200M microscope (White Plains, New York) in the Imaging Core, TTUHSC. The sections were examined for the infiltration of neutrophils, macrophages, and fibroblasts; the presence of edema; and the formation of granulation tissue, neovascularisation, epidermal hyperplasia, and regeneration of hair follicles. For all descriptions of histological findings, "margin" refers to the edge of the wound with adjacent intact skin; "wound bed" refers to the part of the wound from which the skin was removed; and "scab" includes the collection of cells and fluid above the regenerating tissue and immediately beneath the scab itself. As the inflammatory cells were not evenly distributed within the tissue, we counted the numbers of neutrophils within the H&E stained tissue using a standard ocular grid (New York Microscope, Hicksville, New York) or counted cells in the images rendered at 300 dpi within a 300 dpi^2 grid.

2.3.1 | Quantification of wound reepithelialisation and hair follicles

Reepithelialisation of the wounded tissue was evaluated on the H&E stained sections obtained from all groups at 1, 3, and 7 dPIT. We used the muscle layer (panniculus carnosus) as an indicator of the initial wound edges as it is the last to regenerate in the wound healing process. Using a standard ocular grid, the distance from the muscle layer to the end of the regenerating epithelium on one wound edge and the distance between the muscle edges were measured. Percent reepithelialisation was calculated as follows: distance covered by regenerating epithelium/distance between the muscle layers × 100.[28,29] The number of reformed hair follicles was determined by counting the regenerating hair roots in the newly formed epidermis within each tissue section.[30]

2.4 | Construction of panoramic images

Serial images covering the entire tissue section were captured using the Zeiss AxioCAM CCD camera. For construction of the panoramic photomicrograph images, image handling was done with Adobe Photoshop 21.2.4 release (San Jose, California). Individual images were scaled to 300 dpi (4.627 × 3.467 in) followed by auto levels and curves adjustments and the images were matched in sequence. The layers were flattened into one image, which was rotated to a horizontal plane. Counting of cells was carried out on the 300 dpi images. For presentation, compiled images were resized to 600 dpi. Panoramic constructions represent half of the tissue sections obtained at 1, 3, and 7 dPIT. Enlarged companion images taken at ×200 were processed similarly and cells were counted if appropriate. Images were resized to 600 dpi and matched to their respective panoramic. Labelling of images was done in Photoshop.

2.5 | Immunohistochemistry assays

For M1 macrophage staining, the paraffin-embedded sections were sent to the Histology Research Core Facility (University of North Carolina, Chapel Hill, North Carolina) for 3,3′-diaminobenzidine (DAB) staining utilising a pan macrophage primary antibody (F4/80) and iNOS primary antibody.[31,32] For M2 macrophage staining, the avidin-biotin complex method was used.[33,34] Briefly, the paraffin-embedded tissue sections were deparaffinised, rehydrated, and antigen retrieval was done using sodium citrate buffer. All sections were blocked using 20% normal goat serum. The sections were incubated with anti-arginase 1 primary antibody (1:500), washed with phosphate buffered saline (PBS), and incubated with biotinylated goat anti-IgG secondary antibody (1:200). The sections were washed, treated with avidin-biotinylated enzyme complex, and washed a final time. To visualise the M2 macrophages, we utilised a two-component DAB staining kit according to the manufacturer's directions. Sections were counter-stained with haematoxylin and washed in distilled water several times. All sections were visualised under ×100 and ×200 magnification. As a negative control, PBS was used instead of primary antibody. The numbers of M1 and M2 macrophages were determined by counting stained cells using a standard ocular grid; or in the images rendered at 300 dpi, the numbers of stained cells within a 300 dpi^2 grid.

2.6 | Fluorescence-activated cell sorting analysis

Skin tissue harvested from mice with excisional wounds at 1, 3, and 7 dPIT was minced with surgical scissors and digested in RPMI 1640 medium with 0.25% Liberase TL and 0.01% DNase I for 2 hours in an orbital shaking incubator at 70 rpm and 37°C. The samples were passed through sterile 40-μm cell strainers, and single-cell suspensions were re-suspended in RPMI 1640 medium containing 10% fetal bovine serum and penicillin-streptomycin, and then washed in fluorescence-activated cell sorting (FACS) buffer.[35] Cells in each sample were stained with trypan blue and counted using a light microscope. Approximately 1 million cells were added to each well of a 96-well plate and Fc block (1:50) was added. For cell viability, the cells were labelled for 15 minutes at 4°C with SYTOX Green nucleic acid stain, and washed with FACS buffer. The cells were surface-stained for 15 minutes with monoclonal antibodies against CD11b (1:400) and Ly6G (1:1000). Following surface staining, $CD11b^+$ cells were permeabilised with permeabilisation buffer and stained with monoclonal antibodies against iNOS (1:50) or CD206 (1:400). Cells were washed twice with FACS buffer and re-suspended. Samples were run on a BD FACSAria II (BD Biosciences) for data acquisition and analysed with FlowJo software version 7.6.5 (BD Biosciences).

2.7 | C/C analysis

For recovery of proteins, tissues within the wounds produced with 6-mm biopsy punches were excised together with surrounding tissues using 8-mm biopsy punches

and placed in homogenisation tubes containing 1 mL of protein lysis buffer and a protease inhibitor cocktail (1:50). The tissue samples were homogenised and pelleted by centrifugation at 10 000 rpm for 10 minutes at 4°C to obtain a clean supernatant. Protein concentration in each sample was determined using the Bradford assay as previously described.[36] A custom U-PLEX biomarker assay was used to measure the concentrations of six cytokines—IL-6, IL-1β, IL-12p70, IL-17F, GM-CSF, and VEGF-A—and four chemokines—CCL3, CXCL1, CXCL10, and CCL20 within the protein samples according to manufacturer's instructions (Meso Scale Discovery, Rockville, Maryland). Plates were analysed using a MESO QuickPlex SQ 120 (Meso Scale Discovery) that measures electrochemiluminescence. Concentrations of analytes were calculated via standard curves obtained using Discovery Workbench 4.012 software (Meso Scale Discovery).

2.8 | Statistical analysis

Statistical analysis was performed using GraphPad Prism version 9.0.0 (GraphPad Software, San Diego, California, www.graphpad.com). One-way analysis of variance (ANOVA) followed by Tukey's multiple comparisons test was used to determine significant differences between the control and different treatments applied to the wound. Unpaired two-tailed *t* tests were used to compare an individual treatment with its control.

3 | RESULTS

3.1 | BDWG did not delay wound closure

While BDWG eliminated the bioburden within infected wounds,[22] the effect of BDWG on the host response is not known. BDWG may facilitate, have no effect on, or hinder the wound healing process by influencing one or more of the wound healing stages. To examine these possibilities and to delineate the effect of BDWG on host tissue from its antimicrobial effect, we generated full-thickness wounds on the dorsal surface of adult mice.[22,23] In this study, generated wounds were not infected with bacterial pathogens. The wounds were covered with untreated gauze or gauze spread with PEG or BDWG; all wounds were covered with semi-permeable adhesive dressing. At 1, 3, 7, 10, 13, 16, and 19 days PIT, the dressings were carefully removed for physical examination and measurement of wound closure. Regardless of the test group, no evidence of infection was observed and wound closure progressed steadily from 1 dPIT to final closure at 19 dPIT (Figure 2A). There were no significant differences among wound measurements when percent closure at a specific time point was compared among any of the treatments (Figure 2B) or when the surface area (cm^2) of the wounds was compared at the same time points (Figure 2C). Closure of all wounds 19 dPIT suggests that neither PEG nor BDWG significantly delays the wound closure process.

3.2 | BDWG modulated the inflammatory response at 1 dPIT

3.2.1 | BDWG maintained the baseline level of M2 macrophages within the tissue

The numbers of inflammatory cells infiltrating the wounds was determined by FACS analysis using a sequential gating system beginning with CD11b (in the skin, this marker detects neutrophils, M1 and M2 macrophages, and mature natural killer cells), followed by Ly6G (unambiguous detection of neutrophils), and CD206 (separation of M2 macrophages) (Figure 3A). Scatterplots of the sequential gating for all groups at 1, 3, and 7 dPIT are shown in Figure S1. Unfortunately, our attempt to separate M1 macrophages by recognition of iNOS was unsuccessful. However, because natural killer cells are found in very low numbers in normal skin tissue and no eosinophils (which express low levels of CD11b in non-inflamed settings) were seen in any of the H&E stained tissues, the residual $CD11b^+$ cells are most likely M1 macrophages.[37,38,39] Therefore, we subtracted the numbers of neutrophils ($CD11b^+Ly6G^+$ cells) and M2 macrophages ($CD11b^+CD206^+$ cells) from the total number of $CD11b^+$ cells detected to calculate the probable numbers of M1 macrophages ($CD11b^+CD206^-Ly6G^-$) (Table S2). The FACS analysis showed that the percentage of neutrophils was significantly increased over baseline at 1 dPIT in all three treatment groups, increasing from a baseline of 2% in uninjured tissue to ~25% (Figure 3B). Similarly, the percentage of cells within the M1 macrophage pool rose significantly over baseline in all three treatment groups at 1 dPIT (Figure 3C). In contrast to the increase in neutrophils and M1 macrophages, the percentage of M2 macrophages dropped significantly at 1 dPIT from baseline in the UT and PT groups, but remained at baseline (significantly higher than UT and PT) for the BT group (Figure 3D).

3.2.2 | BDWG induced more stable coagulation at 1 dPIT

Over time, the stable fibrin clot that was formed during the haemostasis stage hardens and thickens to form a scab.

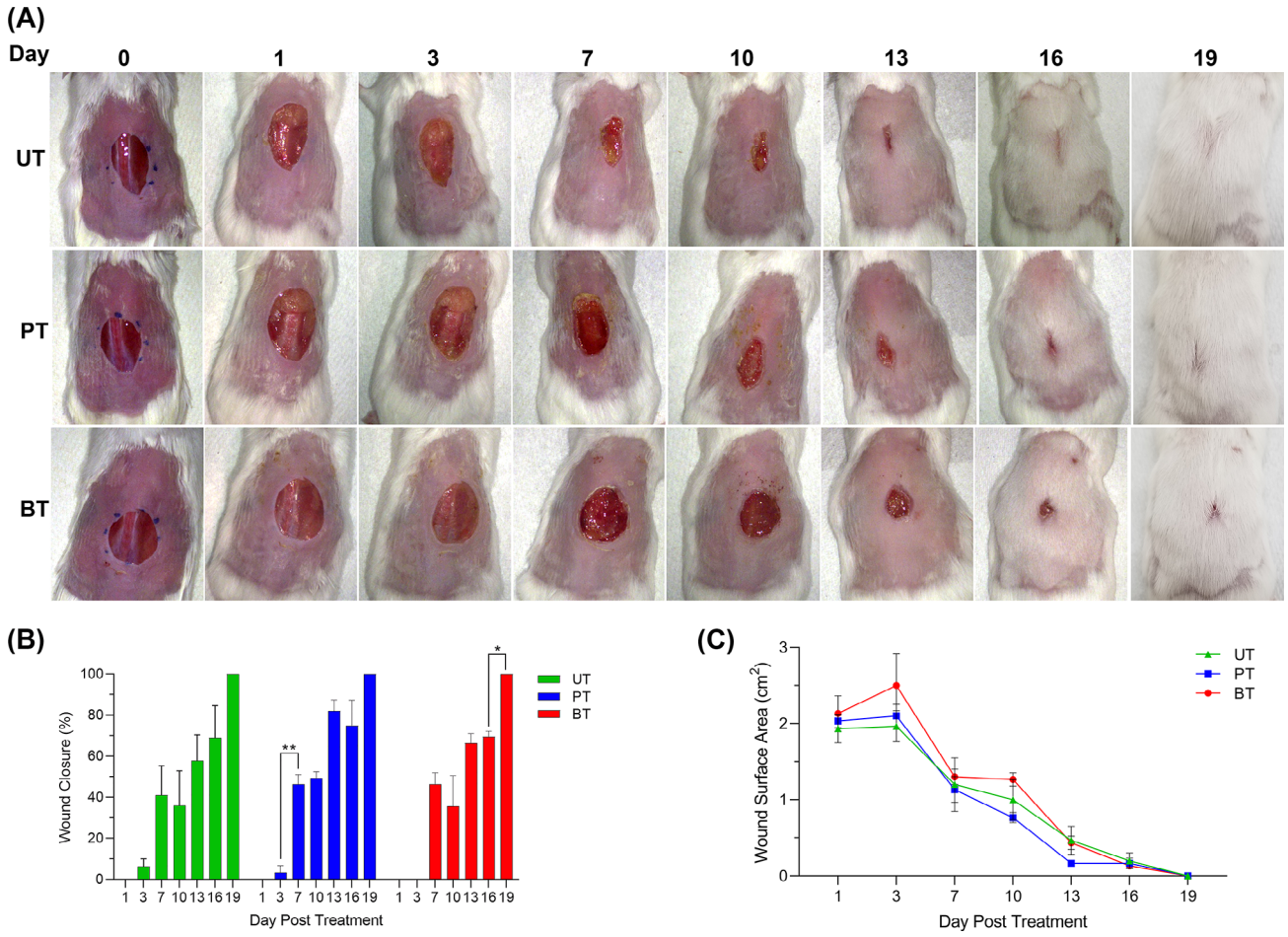

FIGURE 2 Biofilm-dispersing wound gel (BDWG) did not affect wound closure. Full-thickness excision wounds were generated on the dorsum of adult mice (3/group) and were covered with untreated gauze (UT), gauze spread with PEG (PT), or gauze spread with BDWG (BT). All wounds were then covered with transparent adhesive dressing. At 1, 3, 7, 10, 13, 16, and 19 days post-injury/treatment, the adhesive dressings and the gauzes were removed and the wounds examined. A, Macroscopic changes within the skin wounds. All animals were observed for changes of wound appearance. Representative animals were chosen and the same animal was photographed for the series. B, Percentage of wound closure. C, Line graph of the total wound surface area (cm^2). Values in panels B and C represent the means for three animals ± SEM. Significant differences among treatments and from day-to-day changes within a treatment were assessed using two-way analysis of variance (ANOVA) with Tukey's multiple comparisons post-test; *, $P < .05$; **, $P < .01$

Due to the thinness of mouse skin, the tissue excised from the wounds was fragile, especially at 1dPIT and the nascent scabs and provisional matrix tended to separate from the wound margins and beds. Microscopic examination of H&E stained tissue sections revealed the presence of scab fragments over the wounds and initial formation of the provisional matrix, whether UT, PT, or BT (Figure 4). The blood clot was more visible and more cohesive in the BT wounds, extending over the entire surface (Figure 4). These stable clots were present in multiple tissue sections from the three independent experiments, suggesting that they are induced by BT and were not artefacts of the H&E staining.[40] As expected in the inflammatory stage, edema was present in the wound beds of animals receiving all three treatments (Figure 4). Neutrophils were visible throughout the wounds at 1 dPIT, but were most easily visualised infiltrating the wound margins (Figures 4 and 5A). As the neutrophils did not appear to be evenly distributed across the wounds, we counted numbers within the wound margin, wound bed, and the scab (including material directly under the scab) to determine if there were differences in distribution. While there were no significant differences among the treatments, the mean numbers of neutrophils within the grids were highest in the scab (98–122) and lowest in the bed (54–71) at 1 dPIT (Figure 5B). As seen with neutrophils, M1 macrophages were present in the margins, beds, and scabs of the wounds from all three treatment groups (Figures 5D and S2B). While there were

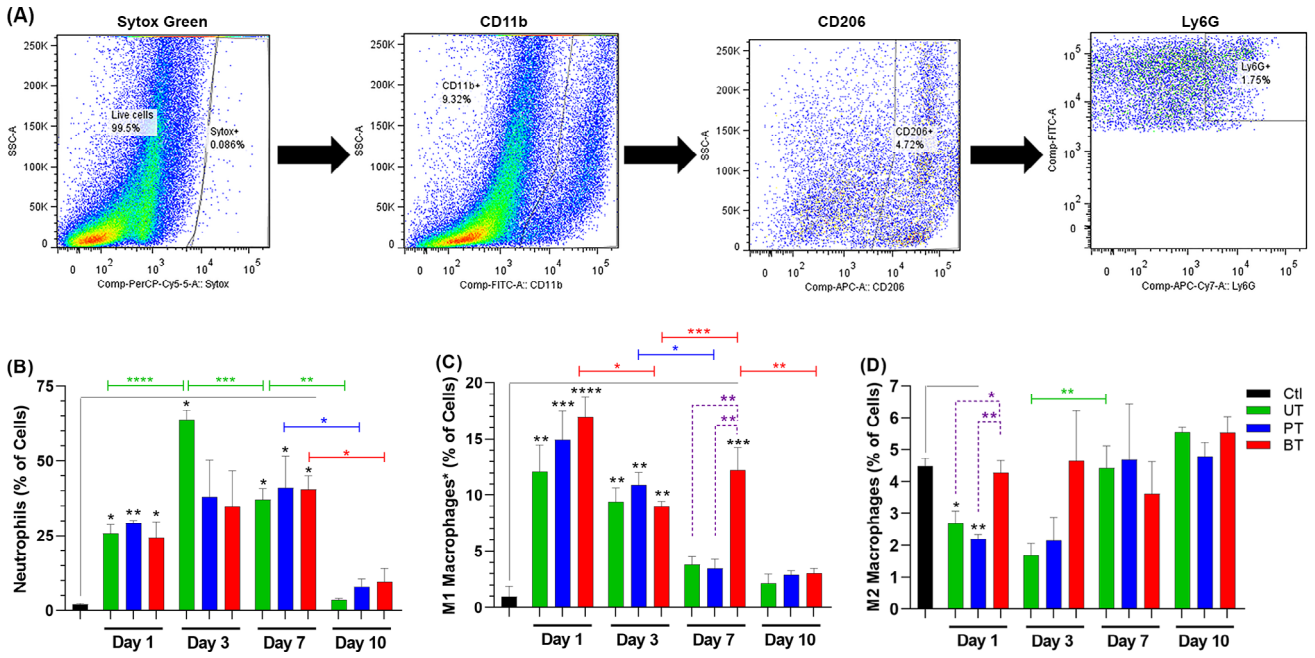

FIGURE 3 Treatment with biofilm-dispersing wound gel (BDWG) does not adversely affect the numbers of inflammatory cells within the wound. Skin tissue from full-thickness excision wounds (three mice/group) was excised and processed for fluorescence-activated cell sorting (FACS) analysis. As baseline controls, the same quantity of skin and associated tissues were harvested from two uninjured mice. A, Sequential gating system for FACS analysis. Scatter plots are representative of the uninjured control group. Live cells were distinguished from dead cells using SYTOX Green nucleic acid stain (Sytox Green); followed by surface staining with anti-CD11b to separate granulocytes (neutrophils, macrophages, and natural killer cells) from other live cells. The $CD11b^+$ cells were internally stained anti-CD206 to separate M2 macrophages followed by internal staining with anti-Ly6G to separate neutrophils. Bar graphs (B-D) show percentages of specific cells within the tissues of uninjured controls and UT, PT, and BT mice. B, Percentage of neutrophils ($CD11b^+Ly6G^+CD206^-$). C, Percentage of $CD11b^+Ly6G^-CD206^-$ cell population that includes primarily M1 macrophages (see text). D, Percentage of M2 macrophages ($CD11b^+CD206^+$). Values represent the means from two mice (Ctl) or three mice (UT, PT, and BT) ± SEM. One-way ANOVA with Tukey's multiple comparisons post-test was used to assess significant differences between baseline control (black bracket and black asterisks), among treatments on each day (dashed purple brackets, purple asterisks), and day-to-day changes within a treatment (colour-coded brackets and asterisks); *$P < .05$; **$P < .01$; ***$P < .001$; ****$P < .0001$. BT, BDWG-treated; PT, PEG-treated; PEG, polyethylene glycol; UT, untreated

no significant differences among the groups, significantly more M1 macrophages were found in the wound margins of BT mice compared with the wound bed/scabs (counted together because of small numbers) (Figure 5D). We also checked for the presence of M2 macrophages. As expected, no M2 macrophages were observed within the wounds from any of the treatment groups at 1 dPIT (Figure S2C).

3.2.3 | BT modulated the expression of proinflammatory C/C

We expected to find increased levels of CCL3, CXCL1, IL-1β, and IL-6, which are secreted by neutrophils and M1 macrophages, as these cells were present in significantly higher numbers compared with the baseline at 1 dPIT (Figure 3B,C). The levels of these four C/C plus GM-CSF within the injured UT, PT, and BT tissues were 6 to 95 times higher than the levels found in uninjured tissues (Figure 6A). The levels of these C/C were higher within the PT tissues than UT, and the levels within BT tissues were lower than UT (Figure 6A). The levels of CXCL1, CCL3, IL-1β, and GM-CSF were significantly lower in the BT tissue than in the PT tissue (Figure 6A). We also observed variations among the BT, PT, and UT groups in the levels of the other C/C—VEGF-A, CXCL10, IL-12p70, IL-17F, and CCL20 (Figure 6A and S3A). Comparisons of the day-to-day changes for each C/C in each treatment group are shown in Figure S3. The full data set and calculations for fold changes can be found in Table S3; graphs of the actual levels (pg/mg) of C/C from each pool are presented in Figure S4.

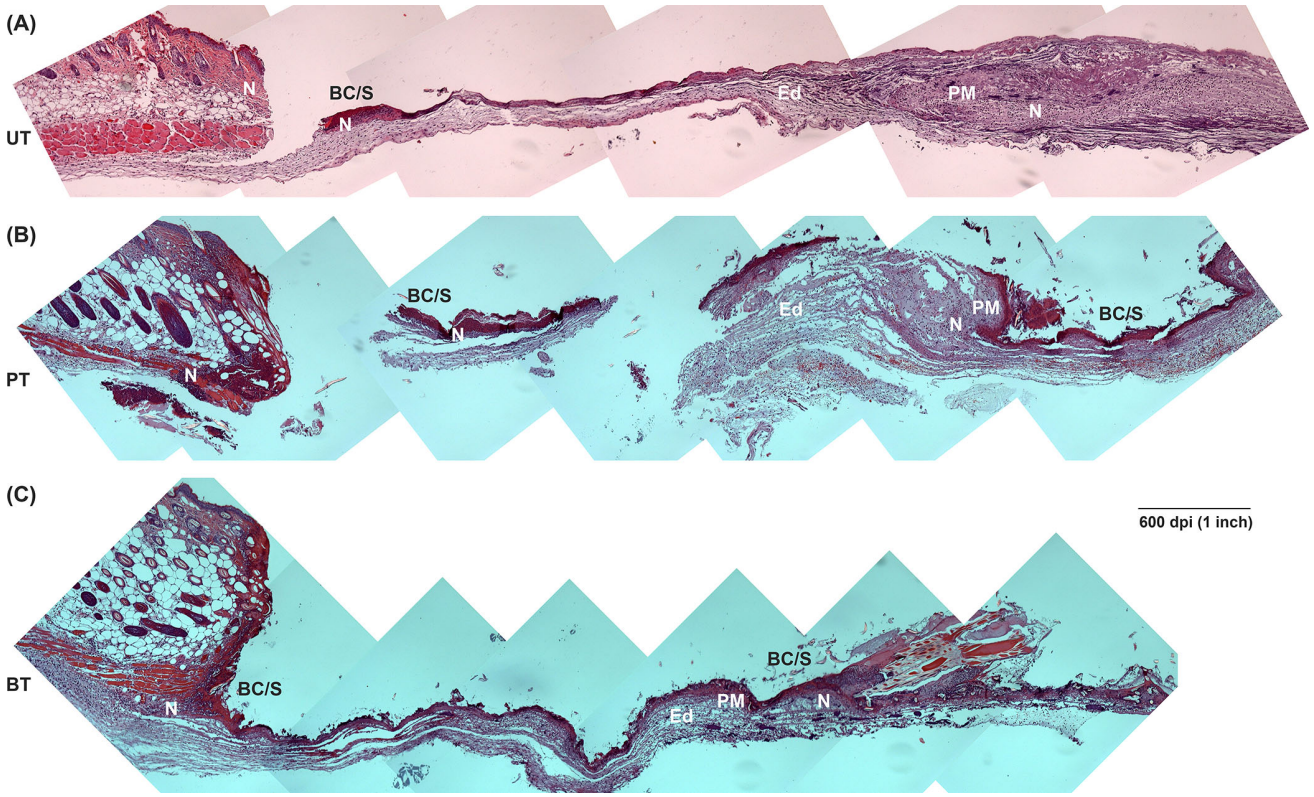

FIGURE 4 Progression of healing at 1 day post-injury/treatment (dPIT). Representative H&E stained tissue sections from wounds of UT, PT, and BT mice were examined for features of the inflammatory stage of wound healing. Serial images of a wound section from one mouse from each treatment group were captured at ×100 magnification using a Zeiss AxioCAM CDD camera and assembled in Photoshop. The panoramic images show half of the wound bed plus normal skin at the wound margin. In some instances, the fragility of the thin wound bed led to breaks and separations during acquisition of the samples, processing of the tissues, or sectioning of the tissues. A, UT wound; B, PT wound; C, BT wound. BT, BDWG-treated; BC/S, blood clot and nascent scab; Ed, edema; H&E, haematoxylin and eosin; N, neutrophils; PM, provisional matrix; PT, PEG-treated; PEG, polyethylene glycol; UT, untreated

3.3 | BT wounds showed more signs of the proliferative stage of healing at 3 days PIT

3.3.1 | Shifts in the inflammatory cell population occurred at 3 days PIT

In uninfected, protected wounds, such as these, the proliferative stage begins between 2- and 3-dPIT. The FACS analysis showed a marked rise to 62% occurred in the levels of neutrophils at 3 dPIT in the UT group while the levels seen in the PT and BT groups rose slightly (Figure 3B). The percentage of cells within the M1 macrophage pool remained significantly higher than baseline at 3 dPIT in all three groups, although the levels had dropped from 1 dPIT (Figure 3C). The drop in M1 macrophages was significant in the BT group (Figure 3C). The levels of M2 macrophages for all three treatment groups changed little at 3 dPIT (Figure 3D).

3.3.2 | BT tissues are more advanced in the proliferative stage

Microscopic examination of the tissues at 3 dPIT revealed signs of the proliferative stage of healing among all three treatment groups. The UT and PT showed thickening of the provisional matrix over the bed of the wound with PT the thickest, but unorganised; while the scab of the BT group was thickened and demarcated from the provisional matrix (Figure 7). The UT wound bed was still edematous (Figure 7A). Epidermal hyperplasia was evident in tissues from all three treatment groups (Figure 7 insets 1, 2 and 4). Quantification of reepithelialisation showed a significant difference between the UT and BT groups (Figure 8A). Significantly more forming hair follicles, another sign of proliferative healing, were found within the BT wounds than in the PT or UT wounds (Figures 7 insets 2 and 4, and 8B). Both reepithelialisation and regeneration of hair

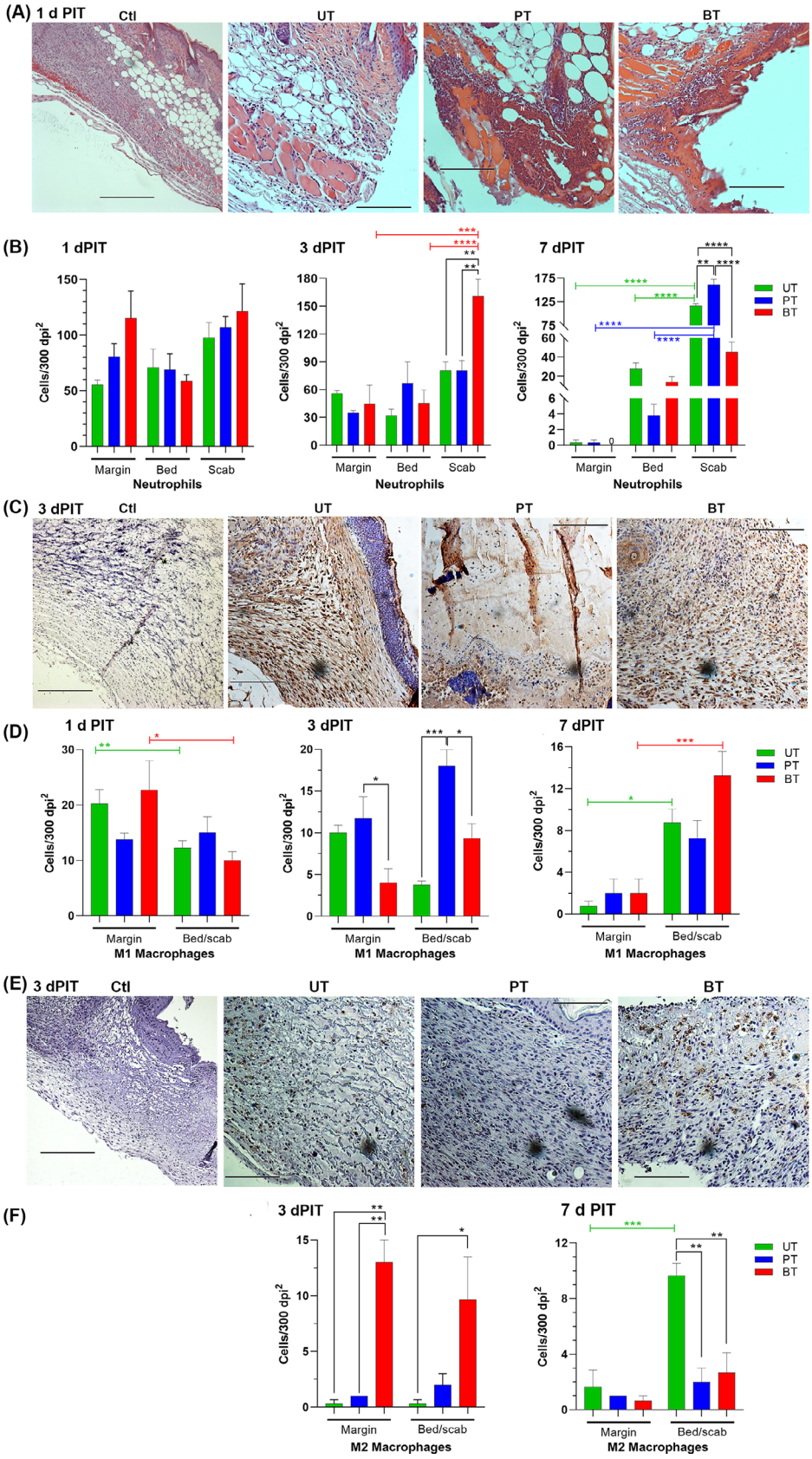

FIGURE 5 Distribution of inflammatory cells within wound margins, beds, and scabs. Photomicrographs are representative of three mice/group and were taken at ×200; bars, 300 dpi. A, Neutrophils stained with H&E are shown at 1 dPIT in uninjured (Ctl) and UT, PT, or BT tissues. B, Distribution of neutrophils within the wound margins, beds, and scabs at 1, 3, and 7 dPIT. C, M1 macrophages stained using iNOS primary antibody and visualised with 3′-diaminobenzidine (DAB) are shown at 3 dPIT. D, Distribution of M1 macrophages. E, M2 macrophages DAB-stained using arginase-1 primary antibody are shown at 3 dPIT. F, Distribution of M2 macrophages. Values on the graphs represent the means of specific cells within 300 dpi^2 grids ± SEM; 3 grids were counted for margins, 6 for wound beds, and 9 for scabs (due to variability). One-way ANOVA was used to detect significant differences between treatments on the same day (no significance) and cell locations within a treatment (coloured brackets); *$P < .05$; **$P < .01$

follicles continue in the remodelling stage of healing. Neovascularisation was also visible in the wound margins and beds of PT and BT mice, but not in those of UT mice (Figure 7 insets 2-5). Additionally, granulation tissue was observed within the bed of BT wounds while reorganised tissue that includes fat cell regeneration can

also be seen (Figure 7C inset 5). While there is strong evidence of advancement into the proliferative stage of healing, the central parts of the wound bed appear to be still within the inflammatory stage. This is likely due to the size of the wound, as closure (evidenced by reduction in size of the wound) did not begin until 7 dPIT (Figure 2).

As at 1 dPIT, neutrophils were present in wounds of all three treatment groups (Figures 3B, 5B and S2A). On 3 dPIT, the total numbers of neutrophils by manual count within the wound margins, beds, and scabs were similar to the totals on 1 dPIT but with significantly higher total neutrophils in the BT group compared with the UT group (Figure S5A). Within the BT group, there was a drop in the neutrophils within the wound margin from 1 dPIT, which was reflected by a rise in the numbers of neutrophils within the scab (Figures 5B, S6A, and S7A). This rise in number of neutrophils beneath the scab was also significantly higher than the numbers found in the UT and PT groups (Figure 5B). The UT group also showed a shift in location of the neutrophils with a drop in the numbers within the wound bed reflected by a significant increase in numbers of neutrophils under and within the scab (Figure S6A). The number of neutrophils in the wound bed of PT mice was higher than those in the margin and lower than those in the scab (Figure 5B). There was a significant drop in numbers of neutrophils in the wound margin of PT mice from day 1 to day 3 (Figure S6A). Similar to the results obtained with flow cytometry, M1 macrophages were observed by immunohistochemistry within the wounds of all three treatment groups (Figure 5C). There was a significant drop in the numbers of M1 macrophages within the wound margins of the UT and BT groups from day 1 to day 3 (Figures S6B and S7B). M1 macrophages were also observed within the wound beds, where the number present in the PT wounds was

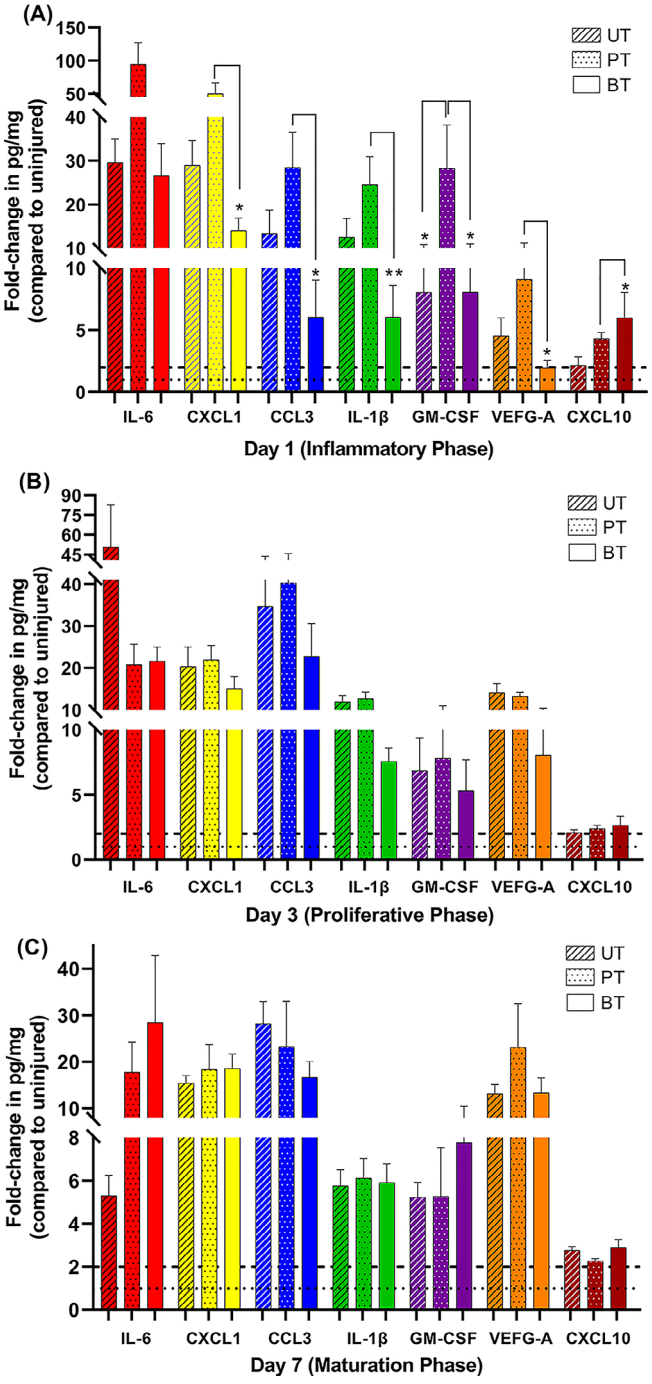

FIGURE 6 Levels of proinflammatory cytokines and chemokines (C/C) are modulated by BDWG. Full-thickness 6-mm punch biopsy wounds were made on the backs of mice (4/group) and the wounds were UT, PT, or BT as described in Figure 2. At 1, 3, and 7 dPIT, tissue from the three biopsy wounds on a single mouse was collected using an 8-mm punch and the tissues were pooled and treated as a single sample (four separate pools/group). An equal amount of tissue was collected from three uninjured mice to serve as baseline for levels of C/C within normal skin. Proteins were extracted from the tissues and concentration of protein in each sample was measured by the Bradford assay. Quantities of the C/C were measured using the U-PLEX biomarker assay with MSD DISCOVERY WORKBENCH software version 4.0; data are reported in pg/mg of protein. Bars represent the means of the fold-change values obtained from the four pools compared with the average value of the uninjured pool (Table S3); striped bars, UT; dotted bars, PT; solid bars, BT. A, Fold changes in levels of IL-6, CXCL1, CCL3, IL-1β, GM-CSF, VEGF-A, and CXCL10 at 1 dPIT; B, Levels of the C/Cs at 3 dPIT; C, Levels of the C/Cs at 7 dPIT. Differences in changes in expression were analysed using one-way ANOVA with Tukey's multiple comparisons post-test; *$P < .05$; **$P < .001$. BT, BDWG-treated; PT, PEG-treated; PEG, polyethylene glycol; UT, untreated

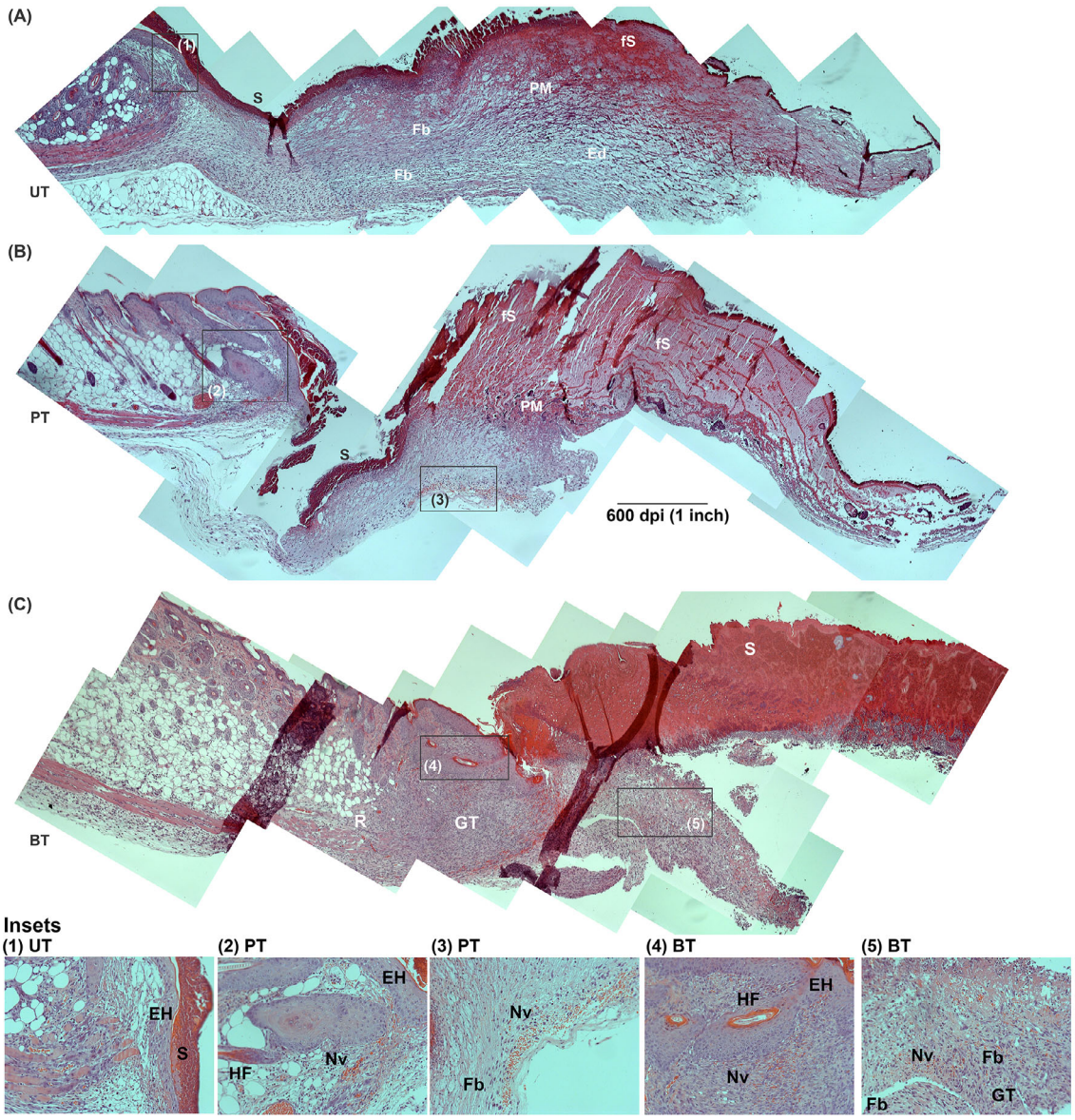

FIGURE 7 Progression of healing at 3 dPIT. Tissue from UT, PT, and BT wounds were H&E stained and examined at ×100 for evidence of inflammatory and proliferative stages of healing. Images were obtained and processed as described for Figure 4. The representative panoramic images show half of the wound bed plus normal skin at the wound margin. Insets indicated by black boxes in panoramas were taken at ×200 and are numbered. A, UT wound with inset 1 showing epidermal hyperplasia; B, PT wound with insets 2 and 3 showing epidermal hyperplasia, regenerating hair follicle, and neovascularisation; C, BT wound with insets 4 and 5. BT, BDWG-treated; Ed, edema; EH, epidermal hyperplasia; Fb, fibroblasts; fS, forming scab; GT, granulation tissue; H&E, haematoxylin and eosin; HF, hair follicle; Nv, neovascularisation; PM, provisional matrix; R, regeneration of fat cells; S, scab; PT, PEG-treated; PEG, polyethylene glycol; UT, untreated

significantly higher than those in the UT or BT wounds (Figure 5D). In accordance with the presence of different stages of healing (proliferative coexisting with maturation), a significant number of M2 macrophages were observed within the wound margins and beds of BT mice compared with UT and PT mice (Figure 5E and F).

3.3.3 | Synthesis of CCL3 and VEGF-A was enhanced at 3 dPIT

At 3 dPIT, we expected that changes in the levels of the 10 C/C would be minimal as the numbers of neutrophils had not reduced, while the number of M1 macrophages had dropped compared with 1 dPIT, and the number of

M2 macrophages had not yet climbed above baseline (Figures 3 and S5). Additionally, keratinocytes, fibroblasts, myofibroblasts, vascular endothelial cells, and other cells present within the wound margin and bed were expected to contribute to the C/C concentrations. The levels of CCL3, VEGF-A, and IL-17F all rose from 1 dPIT to 3 dPIT in UT, PT, and BT tissues with the levels of CCL3 increasing to 35-, 40.5-, and 23-fold over baseline, respectively (Figures 6B and S3B). The levels of VEGF-A rose more modestly (Figure 6B) and were accompanied with visible neoangiogenesis within the PT and BT tissues (Figure 7B and C). The baseline level for IL-17F, at 1206 pg/mg, was the highest level of any of the 10 C/C found within the uninjured tissue; therefore, the modest increases found (UT from −0.5- to 1.5-fold; PT from 0.07- to 1.4-fold; BT from −1.3- to 1.3-fold) represent an increase of 400 to 600 pg/mg of tissue (Figure S4B and Table S3). Protein levels were more variable for the other C/C—IL-6, CXCL1, IL-1β, GM-CSF, CXCL10, IL-12p70, and CCL20 (Figures 6B and S4).

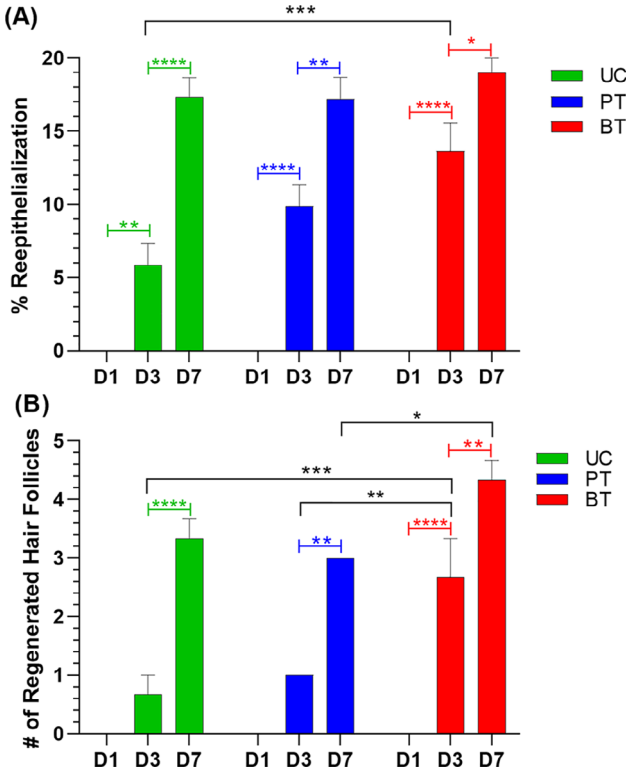

FIGURE 8 BDWG stimulates reepithelialisation and hair follicle regeneration at 3 dPIT. H&E stained tissue sections of UT, PT, and BT wounds at 1, 3, and 7 dPIT were examined for reepithelialisation and regeneration of hair follicles using an ocular grid. The fully-formed panniculus carnosus was used to locate the original wound margin in the healing wounds. A, Percentage of reepithelialisation of the wound. B, The number of hair follicles formed within healing tissue. Values represent the counts from stained sections obtained from three mice ± SEM. One-way ANOVA was used to detect significant differences between treatments on the same day (black brackets) and within a treatment on different days (coloured brackets); *$P < .05$; **$P < .01$; ***$P < .001$; ****$P < .0001$. BDWG, biofilm-dispersing wound gel; BT, BDWG-treated; H&E, haematoxylin and eosin; PT, PEG-treated; PEG, polyethylene glycol; UT, untreated

3.4 | BT wounds show a continuum of healing at 7 dPIT

3.4.1 | Inflammatory cells were present at 7 dPIT

The percentage of neutrophils remained significantly increased over baseline at 7 dPIT in all three treatment groups by FACS analysis (Figure 3B). As this suggests persistence of the inflammatory stage, we examined the

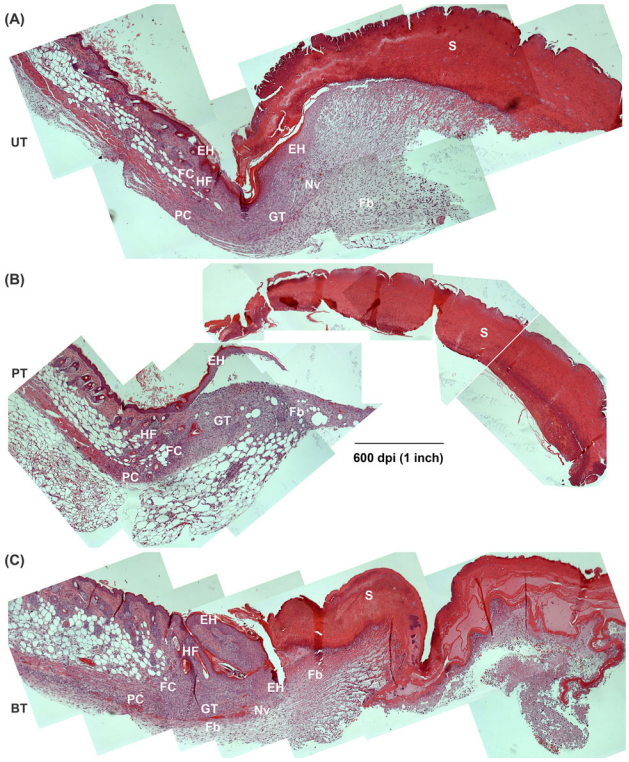

FIGURE 9 Progression of healing at 7 dPIT. Tissue from UT, PT, and BT wounds were H&E stained and examined at ×100 for evidence of inflammatory, proliferative, and remodelling stages of healing. Images were obtained and processed as described for Figure 4. The representative panoramic images show half of the wound bed plus normal skin at the wound margin. A, UT wound; B, PT wound; C, BT wound. BT, BDWG-treated; Ed, edema; EH, epidermal hyperplasia; Fb, fibroblasts; FC, new fat cells; GT, granulation tissue; H&E, haematoxylin and eosin; HF, hair follicle; Nv, neovascularisation; PC, regenerating panniculus carnosus; PT, PEG-treated; PEG, polyethylene glycol; S, scab, UT, untreated

levels of neutrophils at 10 dPIT. At this time point, the levels of neutrophils in all treatment groups were no longer significantly increased over baseline, dropping to 10% or less (Figure 3B). At 7 dPIT, the levels of M1 macrophages in the UT and PT groups were significantly lower than that of the BT group, which remained significantly higher than baseline (Figure 3C). By 10 dPIT, the levels of M1 macrophages in all three groups had returned to just above baseline (Figure 3C). At 7 dPIT, the levels of M2 macrophages were near baseline for all three groups, and by 10 dPIT, the levels were slightly higher (Figure 3D).

3.4.2 | Overlap in inflammation, proliferation, and remodelling

Very dynamic changes were observed within the wounded tissues of all three treatment groups. The scabs of the UT and PT groups were now similar to that of the BT group and granulation tissue was observed in all three wound treatments (Figure 9). Reepithelialisation was further advanced in all three groups and was approximately equal (Figures 8A and 9). While the numbers of hair follicles had also increased in all three treatment groups, the increase in hair follicles was significantly higher in BT compared with PT (Figure 8B). Neovascularisation was now prominent in the UT and BT groups but less so in the PT group (Figure 9). Additionally, there was regeneration of fat cells and initial regeneration of the panniculus carnosus at the margins of all three wounds (Figure 9). Neutrophils were still present within the wounds of all three treatment groups, primarily visible within and under the scabs (Figures 5B and S2A). M1 macrophages were also found mainly within the wound beds/scabs (Figures 5D and S2B) while M2 macrophages were present in low numbers within the granulation tissue (Figures 5E and S2C).

Once again, the population of inflammatory cells had shifted within the tissues of all three treatment groups. Neutrophils disappeared from the healing margins and were found in higher numbers in the wound bed in the UT group (mean 35) compared with the PT and BT groups (means 3 and 14, respectively) (Figure 5B). The numbers of neutrophils within and under the scab of the BT group were significantly lower than in the PT and UT groups (Figure 5B). This number was also significantly reduced from the number seen at 3 dPIT in the BT wound (Figure S6A). The PT group showed a significant increase in neutrophils within the scab compared with 3 dPIT and compared with the wound bed and margin (Figure S6A), suggesting continuation of the inflammatory stage even at 7 dPIT. All three groups showed significant shifts in the neutrophil population from the margin to the bed to the scab (Figure S6A). The population of M1 macrophages in the wound margins and beds were similar in all three treatment groups (Figure 5D). However, the population of M1 macrophages decreased significantly from 3 to 7 dPIT in the margins and beds of the PT group and the margins of the UT group (-Figure S6B). No significant shifts in M1 population were observed in the BT group (Figure S6B). Among the treatment groups, the numbers of M2 macrophages observed at 7 dPIT were similar in the wound margins of all three groups and in the wound beds of the PT and BT groups (Figure 5F). The population of M2 macrophages increased dramatically in the wound beds of the UT group at 7 dPIT (Figure S6C). In contrast, there was a significant decrease in the numbers of M2 macrophages present in the wound margins of BT mice and a decrease in the mean numbers in the wound beds from 10 to 3 (Figure S6C).

3.4.3 | IL-6 and GM-CSF increased in BT wounds

Non-infected wounds in mice usually enter the maturation/remodelling stage of wound healing by 7 dPIT. Therefore, we expected to see a reduction in protein levels of CCL3, IL-6, and IL-1β; C/C considered "inflammatory" in nature. While the levels of all three were reduced from 3 dPIT, the levels of CCL3 remained high at 28-, 23-, and 17-fold over baseline in the UT, PT, and BT tissues, respectively (Figure 6C). The level of IL-6 dropped precipitously in the UT tissues, from 50-fold over baseline at 3 dPIT to only 5-fold at 7 dPIT; a modest drop was seen in the PT tissue and the level in BT tissue rose to 28-fold over baseline (Figure 6C). The continued expression of IL-6 may be accounted for by the presence of fibroblasts (Figure 9C) and the activity of M2 macrophages, which were slightly over baseline in all tissues (Figure 3D). The levels of CXCL1, VEGF-A, GM-CSF, and CXCL10—C/C indicative of the shift from proliferation to maturation—remained at least 2-fold above baseline synthesis in all tissues from all three treatments (Figure 6C). The levels of CXCL1, CXCL10, and VEGF-A rose in BT tissues at 7 dPIT compared with 3 dPIT (Figure 6C). The levels of CCL20 remained below baseline (−2.8, −3.1, and −3.5-fold) in all the UT, PT, and BT groups, respectively (-Figure S3C). These results suggest that neither PEG nor BDWG interferes with the wound healing process. It is likely that the continued higher levels of some C/C represent the continuum of healing going on within the wound.

4 | DISCUSSION

The most critical features of ideal wound management products are that they prevent infection or significantly reduce or eliminate the wound bioburden; and that they promote the wound healing process or, at least, do not interfere with it. Different wound management products vary in their ability to fulfil those critical criteria. Using the murine model of wound infection, we previously demonstrated that BDWG (once known as G5 wound gel) is a strong broad-spectrum antimicrobial.[22] In both in vitro and in vivo models, Miller et al[22] demonstrated that BDWG eliminated biofilms established by either *Staphylococcus aureus* or *Pseudomonas aeruginosa*. In this study, using a model of non-infected wounds, none of the three treatments delayed wound closure (Figure 2). However, each treatment had subtle effects on the histology, cellular infiltration, and cytokine/chemokines in the healing wounds.

4.1 | The influence of the treatments on the stages of wound healing

4.1.1 | The haemostasis and inflammation stages

The formation of a stable blood clot provides both protection of the wound and a matrix in which immune cells can gather to orchestrate the healing process.[3,4,40] Blood clots and nascent scabs were present in tissues from UT, PT, and BT wounds (Figure 4). However, those in the PT wounds were friable and easily disrupted while those in the BT wounds were more durable and less likely to fragment, suggesting that the BT group has completed secondary haemostasis ahead of the PT group. Blood clots in the UT wounds were similar to those in the BT group, but less pronounced and still somewhat fragile. The presence of blood clots at 1 dPIT has been reported previously. Using a murine model of wounds, Kim et al observed blood clots in injured mice at 1 day post-injury.[41] In a normal animal, the first stage of haemostasis (coagulation) begins within 1 to 9 minutes and coagulation is usually complete within 1 hour.[42]

As haemostasis proceeds, the inflammatory stage begins, marked by the appearance of edema within the tissue, infiltration of immune cells, and secretion of proinflammatory cytokines.[2,16,43] Consistent with this description, edema was observed in the wound beds of all treatment groups. The amount of edema within the PT wounds appeared much more substantial than within the UT or BT wounds (Figure 4), which may explain why the tissue from PT wounds was more easily fragmented. As expected, neutrophils were found infiltrating the wounds of all treatment groups in similar numbers (Figures 3B and S5A). Similarly, the levels of the proinflammatory C/C IL-6, CXCL1, CCL3, IL-1β, and GM-CSF were elevated above the baseline found in normal uninjured murine skin in tissues from all three wound treatments but were highest in the PT wounds (Figures 6A and S4A-E). The high levels of C/C present in the PT wounds may be responsible for the increased amount of edema within the tissues. In contrast, the levels of CXCL1, CCL3, IL-1β, and GM-CSF were significantly lower in the BT wounds compared with the PT wounds, suggesting a more modulated inflammatory response within the BT wounds. Interestingly, the levels of CXCL10, a chemokine usually observed later in the wound healing process that activates monocytes and macrophages for the reparative roles in healing, were significantly higher in BT wounds (Figure 6A).[44,45] Because the level of M1 macrophages was significantly elevated at 1dPIT, and the level of M2 macrophages was at baseline (and significantly higher than the levels seen in UT and PT tissues) (Figure 3), these cells could have played a role in the production of CXCL10. The presence of the components of BDWG in PEG eliminated the PEG-induced increases in C/C production. The levels of IL-6 and GM-CSF within the wounds of the BT group were similar to the UT group, and the levels of CXCL1, CCL3, and IL-1β were lower (Figure 6). The presence of benzalkonium chloride in the BDWG could potentially be responsible for eliminating the effect of PEG treatment on the wounds. A recent study showed that treatment with benzalkonium chloride has a potentially beneficial effect on wound healing. In a rat excisional wound model, treatment with benzalkonium chloride improved the wound healing rate and reduced the cellular infiltrate.[46]

4.1.2 | Proliferative stage

At 3 dPIT, and as inflammation subsides, the proliferative stage begins and may last up to 2 weeks post-injury.[47,48] The proliferative stage is characterised by three connected steps: (a) reepithelialisation, (b) angiogenesis, and (c) formation of granulation tissue.[12,17,48,49] At 3 dPIT, the histology of the three treatment groups varied the most. Wounds of the UT group were covered by forming scabs with adjacent provisional matrix, the wound beds were still edematous (Figure 7A), the infiltrating neutrophils had increased to 64%, and the number of M1 and M2 macrophages had dropped below the baseline (Figure 3). There was a concomitant increase in IL-6 and CCL3 (Figure 6B). Despite these indications of inflammation, there was evidence of epidermal hyperplasia and

reepithelialisation (Figures 7A and 8A), suggesting that the wounded tissues are in a continuum of healing between the late stages of inflammation and the earliest part of the proliferative stage. This delay in the transition is likely due to the lower number of M1 macrophages, which trigger neutrophils to undergo apoptosis and then ingest them (efferocytosis).[7,8,10] Previous studies have shown that in a murine wound model the absence of M1 macrophages leads to an increased level of neutrophils within the wound.[50,51] The increased level of neutrophils prolongs inflammation by increasing the level of proinflammatory cytokines IL-6 and IL-1β.[50,51] Continuation of the inflammatory wound environment prevents secretion of anti-inflammatory cytokines that, together with M1 neutrophil efferocytosis, are needed to increase the numbers of M2 macrophages within the wound.[7,50,52] Additionally, Dovi et al[53] observed that in a murine wound model, high levels of neutrophils can impair the wound repair process by delaying the reepithelialisation of wounds. Further evidence for the delay in the transition to the proliferative stage was the low level of reepithelialisation (about 5%) (Figure 8A), which is considerably lower than the previously reported 33%.[53-56] One possible reason for this difference is the variation in the excision wound surface area. Compared with our 1.5 cm^2 full-thickness wound, other studies induced smaller ones (6-8 mm in diameter).[53-56] Smaller wounds are likely to heal faster than larger ones and the wounded tissues may enter the proliferative stage earlier.

Similar to the UT group, the PT group is also on the continuum between the late stages of inflammation and the early stages of proliferation, although the healing tissue appeared disorganised except close to the wound margin where neovascularisation, epidermal hyperplasia, and reepithelialisation were observed (Figures 7 and 8A). The level of neutrophils was considerably lower than in the UT wounds (38% vs 64%) (Figure 4B). The lower infiltration of neutrophils, which reduced the amount of neutrophil secreted proteases within the wound, may have allowed for neovascularisation to proceed.[7,57,58] Despite that, signs indicative of delayed proliferation including low reepithelialisation rate (10%), a low level of M2 macrophages (2%), and continued expression of proinflammatory C/C above baseline (Figures 3D, 8A and 6B).

At 3 dPIT, BT had a positive impact on wound healing at 3 dPIT by promoting aspects of the proliferation stage, including epidermal hyperplasia, significant hair follicle formation, regeneration of fat cells, neovascularisation, the presence of granulation tissue, and a significant amount of reepithelialisation (compared to UT and PT wounds) (Figures 7C and 8A). The percentage of neutrophils was even lower than PT (35%), and the levels of the proinflammatory C/C were also reduced or remained similar to the levels found at 1 dPIT (Figure 6B).

4.1.3 | Remodelling stage

In an uninfected wound, the remodelling (or maturation) stage of healing begins by 7 dPIT and is signified by replacement of granulation tissue with cellular matrix, continued cell proliferation, synthesis of new extracellular matrix molecules, and angiogenesis.[13,59] In UT wounds at 7 dPIT, the level of neutrophils was reduced to 37% (compared with 64% at 3 dPIT) but was still higher than it was at 1 dPIT (26%) (Figure 3B). Previous studies utilising the murine wound model have reported reductions to as low as 20% by 7 dPIT.[18,53] The neutrophils remaining within the wound may facilitate the wound healing process by secreting matrix metalloproteases that degrade collagen and fibronectin, thereby facilitating the remodelling of the wounded tissue.[60] As discussed above, the surface area of the excision wounds generated differs in multiple studies, a factor likely influencing the number of infiltrating neutrophils; wounds with a smaller surface area contain fewer infiltrating neutrophils. Indeed, when we analysed the wounds at 10 dPIT, they were much smaller than those at 7 dPIT and the number of infiltrating neutrophils was reduced by 10-fold from 37% to 3.6% (Figure 3A). Concomitant with the reduction in neutrophils, and as further evidence that the inflammation is resolving, there was a reduction in the level of all five proinflammatory C/C (IL-6, CXCL1, CCL3, IL-1β, and GM-CSF), although none were below baseline (CCL3 was the highest at 28-fold over baseline) (Figures 6C and S4A-E). Consistent with entry into the remodelling stage, we observed extensive epidermal hyperplasia with reepithelialisation enhanced significantly, more regeneration of hair follicles, and regeneration of fatty tissue and the panniculus carnosus at the wound margins (Figures 8 and 9A). However, the level of reepithelialisation (about 15%) (Figure 8A) was considerably lower than that reported by previous studies.[28,53-56] Using a similar murine model of excision wound, Low et al[54] observed a high level of reepithelialisation (60%) at 7 dPIT. We also detected several features that suggest the UT wounds were also in the proliferative stage, including the presence of neovascularisation, granulation tissue, and M2 macrophages (Figures 3D and 7B). Overall, these observations suggest that in our model of

wound excision with its large wound surface area, wound healing at 7 dPIT encompasses a continuation of the proliferative stage along with entry into the remodelling stage.

Similar to the UT group, the PT group showed signs of full entry into the proliferative stage; mature scab, formation of granulation tissue, more extensive neovascularisation, and a drop in M1 macrophages with an increase in M2 macrophages (Figures 3 and 9B). Additionally, there was more extensive epidermal hyperplasia and reepithelialisation, regeneration of fatty tissue and the panniculus carnosus, further restoration of hair follicles, and a decrease in levels of the five proinflammatory C/C (Figures 6C, 8 and 9B).

At 7 dPIT, the BT group showed most clearly that healing of a large surface wound proceeds along a continuum rather than entering discreet stages. At the wound margins, remodelling had occurred with development of an almost normal epidermal layer (less hyperplasia), more extensive reepithelialisation, resolution of neovascularisation, and regeneration of fatty tissue, the panniculus carnosus, and hair follicles (Figures 8 and 9C). The wound bed adjacent appeared to be in the proliferative stage with epidermal hyperplasia, granulation tissue formation, and neovascularisation occurring closer to the centre of the wound (Figure 9C). Manual examination of the tissue showed a decrease in neutrophils, the majority of which were associated with the scab (Figures S5A and S7A). Unlike the UT and PT groups, the levels of the proinflammatory C/C varied considerably. The levels of CCL3 and IL-1β decreased, while the levels of IL-6, CXCL1, and GM-CSF increased (Figure 6C). The presence of neutrophils and the levels of C/C suggest that inflammation is still occurring near the centre of the wound at 7 dPIT. Alternatively, the elevation in IL-6 may be related to the progression of the BT wounds into the later stages of healing. Although it contributes to the recruitment of neutrophils and macrophages, recent analyses showed that IL-6 also facilitates wound healing at late stages of the wound healing process by organising collagen.[28,43] Lin et al[28] observed that in *Il6* knockout mice, collagen formation was disorganised and the wound healing was delayed, whereas in the wild-type mice, the collagen formation was organised and the wound closure rate had increased. Similarly, a role for GM-CSF in the remodelling stage of healing has been demonstrated in a hamster model of corneal healing,[61] a rabbit model of vocal fold healing,[62] and healing of chronic wounds in humans.[63] Thus, the increase in GM-CSF seen in the BT wounds likely played a role in the observed tissue remodelling.

4.2 | Changes related to PEG only

Previous studies showed that PEG-based hydrogels (without the addition of an antimicrobial agent) help maintain a moist environment within the wound, which facilitates the wound healing process by preventing tissue dehydration.[25,64] Besides this, the moist environment provided by the PEG-based hydrogels has been shown to accelerate angiogenesis, the breakdown of dead tissues and fibrin, and strengthen the interaction of growth factors with their targets.[64,65] Furthermore, PEG-based hydrogels have been shown to enhance the wound closure process.[25] In our model, PT mice showed no signs of toxicity (data not shown) and neither erythema nor irritation was seen in the healthy skin around the wound (Figure 2). Compared with the UT group, PT did not significantly alter wound closure or reepithelialisation rates (Figures 2 and 8A). Despite that, and at specific time points post-treatment, PEG still affected certain aspects of the wound healing process. Compared with UT wounds, there was more edema in the wound bed at 1 dPIT; more M1 macrophages at 3 dPIT with more remaining in the wound bed, more neutrophils within the wound bed at 3 dPIT, and higher levels of proinflammatory C/C at 1 dPIT.

4.3 | BDWG compared with other topical antimicrobials

Using murine models of wound infections, previous studies assessed the effect of topical antimicrobials, including antibiotics and silver, on different aspects of the wound healing process. Hwang et al[66] examined the effect of cross-linked hydrogel films with polyvinyl alcohol, dextran, and 0.1% gentamicin on wound healing. Compared with gauze alone, conventional product, and hydrogel film without gentamicin, the hydrogel film with gentamicin enhanced reepithelialisation, decreased the level of inflammatory cells within the wound, and accelerated remodelling of the granulation tissue at 15 dPIT.[66] Although we examined the wounded tissue at much earlier time points, BT treatment also enhanced reepithelialisation, decreased numbers of inflammatory cells, and produced a more organised appearance within the healing tissue sooner than UT or PT. Numerous commercially-available silver-based wound dressings have been examined for their effect on wound healing. In one study, Thomason et al[67] assessed the effectiveness of a silver oxysalt dressing in promoting the healing of non-infected incisional cutaneous wounds. At 3 dPIT, silver oxysalt dressing significantly advanced reepithelialisation

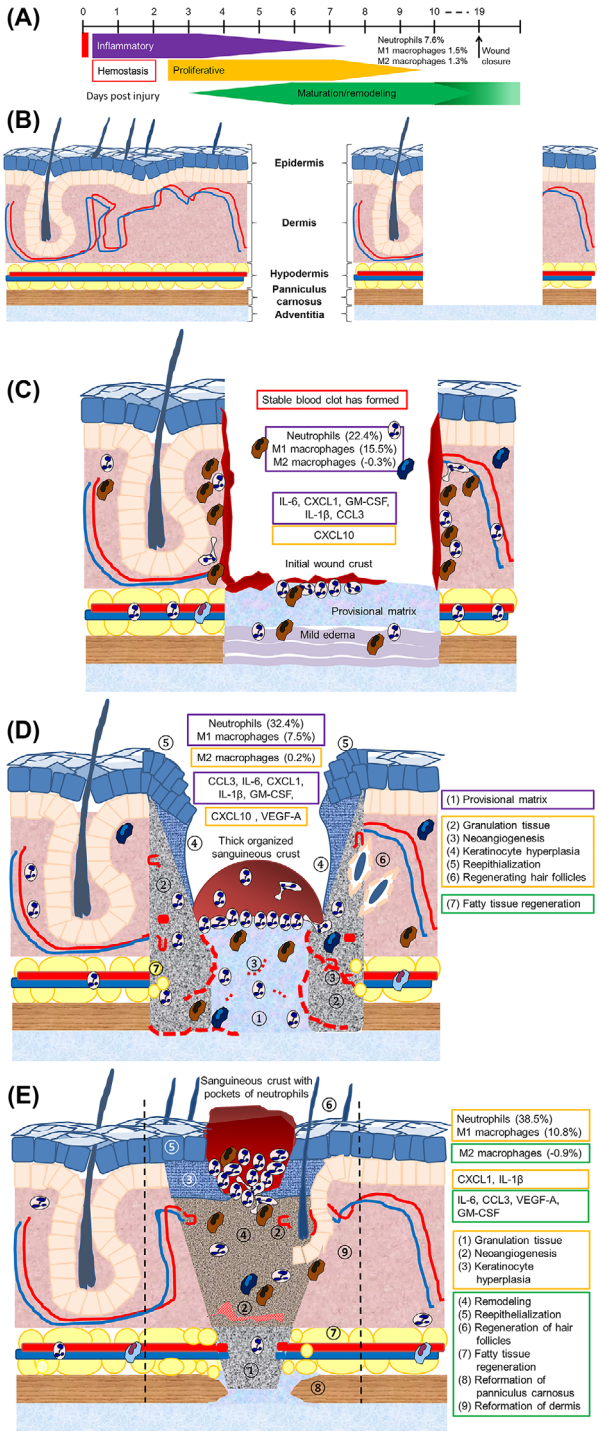

FIGURE 10 Model summarising the effect of BDWG on wound healing. A, Revised timeline showing the continuum of healing observed in the BT wounds. B, Diagram of normal skin and the excision wound imposed on normal skin. Progression of healing from 1 dPIT (C) to 3 dPIT (D) to 7 dPIT (E) showing key findings at each stage of healing. Boxes in C, D are colour-coded to match the stages of healing shown in A (red, haemostasis; purple, inflammatory; orange, proliferative; green, remodelling). Features of each stage of healing are indicated by numbered circles on diagrams D and E. Dashed lines on panel E indicate the original margins of the wound. BDWG, biofilm-dispersing wound gel; BT, BDWG-treated

compared with the control group; but by day 7 after wounding, the wounds in both groups were fully epithelialised.[67] At both 3 and 7 dPIT, wounded tissues treated with silver oxysalt contained significantly higher neutrophil and macrophage infiltrate than the control.[67] Similar to the effect of silver oxysalt, BT wounds showed significantly advanced reepithelialisation compared with the control groups at 3 dPIT, while the percentage of reepithelialisation was similar in all treatment groups at 7 dPIT (Figure 8A). At 3 dPIT, more neutrophils were found within the margins, beds and scabs of the BT wounds than the UT wounds (82/grid versus 69/grid), but at 7 dPIT this was reversed, with a significant reduction in neutrophils in the BT wounds (28/grid versus 103/grid) (Figure S5A). Similarly, the BT wounds contained significantly fewer M1 (inflammatory) macrophages at 3 dPIT and significantly more M2 (healing) macrophages (Figure S5B and C).

5 | CONCLUSION

In this study, we demonstrated that BDWG did not interfere with the wound closure rate, did not adversely affect the healthy skin around the wound (no erythema or staining), and caused no delay in progression through the four stages of the wound healing process (Figure 10A). Indeed, the BT wounds were found to be in a continuum of healing in which the inflammatory stage overlapped considerably with the proliferative stage and the remodelling stage began during the proliferative stage (Figure 10A). At 1 dPIT, BT wounds were covered with a stable blood clot, had less edema in the wound bed, and the levels of proinflammatory C/C were elevated but were still low enough to prevent excess fluid accumulation and inflammatory cell influx (Figure 10C). At 3 dPIT, BT facilitated reepithelialisation of the wounded tissues, regeneration of hair follicles, neovascularisation within the wound margins and beds, and reduced the number of neutrophils; the majority of the neutrophils had migrated to the scab where their proteases would be most helpful in remodelling the healing wound tissue (Figure 10D). By 7 dPIT, healing appeared more organised and advanced with portions of scab gone from the reepithelialised wound surface (Figure 10E). Because the wounds were not infected, these outcomes are due to the BDWG itself rather than the eradication of a wound bioburden. Collectively, data from this study and our previous study[22] strongly suggest that BDWG fulfils the two critical criteria for an effective antimicrobial topical application to treat infected wounds; it eliminated the wound bioburden and did not interfere with different aspects of the wound healing process. Beyond its non-interference,

treatment of the wounds with BDWG enhanced healing, especially at 3 dPIT.

ACKNOWLEDGEMENTS

The authors thank Kathryn L. Furr for her invaluable assistance with the FACS analysis. The authors also thank Joanna E. Swickard for critical reading of this manuscript.

CONFLICT OF INTEREST

K.B. was funded by a graduate student research support award from the Texas Tech University Graduate School, the Texas Tech Chapter of the American Society for Microbiology, the Texas Tech Association of Biologists, and in part by Next Science, LLC (Jacksonville, Florida). M.M. is the Chief Technology Officer for Next Science, LLC. The funding source had no role in the collection, analysis, or interpretation of data, in the writing of the manuscript, or in the decision to submit the paper for publication. J.A.C-H., R.M.J., and A.N.H. have no conflicts of interest.

DATA AVAILABILITY STATEMENT

The data that supports the findings of this study are available in the supplementary material of this article.

ORCID

Jane A. Colmer-Hamood https://orcid.org/0000-0002-3768-5168
Matthew Myntti https://orcid.org/0000-0003-0520-1189
Abdul N. Hamood https://orcid.org/0000-0001-7193-7827

REFERENCES

1. Diegelmann RF, Evans MC. Wound healing: an overview of acute, fibrotic and delayed healing. *Front Biosci*. 2004;9:283-289.
2. Gonzalez AC, Costa TF, Andrade ZA, Medrado AR. Wound healing—a literature review. *An Bras Dermatol*. 2016;91(5):614-620.
3. Golebiewska EM, Poole AW. Platelet secretion: from haemostasis to wound healing and beyond. *Blood Rev*. 2015;29(3):153-162.
4. McMichael M. Primary hemostasis. *J Vet Emerg Crit Care*. 2005;15(1):1-8.
5. Barrientos S, Stojadinovic O, Golinko MS, Brem H, Tomic-Canic M. Growth factors and cytokines in wound healing. *Wound Repair Regen*. 2008;16(5):585-601.
6. Eming SA, Krieg T, Davidson JM. Inflammation in wound repair: molecular and cellular mechanisms. *J Invest Dermatol*. 2007;127(3):514-525.
7. Koh TJ, DiPietro LA. Inflammation and wound healing: the role of the macrophage. *Expert Rev Mol Med*. 2011;13:e23.
8. Landén NX, Li D, Ståhle M. Transition from inflammation to proliferation: a critical step during wound healing. *Cell Mol Life Sci*. 2016;73(20):3861-3885.
9. Su Y, Richmond A. Chemokine regulation of neutrophil infiltration of skin wounds. *Adv Wound Care*. 2015;4(11):631-640.
10. Wynn TA, Vannella KM. Macrophages in tissue repair, regeneration, and fibrosis. *Immunity*. 2016;44(3):450-462.
11. Italiani P, Boraschi D. From monocytes to M1/M2 macrophages: phenotypical vs. functional differentiation. *Front Immunol*. 2014;5:514.
12. Tonnesen MG, Feng X, Clark RA. Angiogenesis in wound healing. *J Investig Dermatol Symp Proc*. 2000;5(1):40-46.
13. Rodero MP, Khosrotehrani K. Skin wound healing modulation by macrophages. *Int J Clin Exp Pathol*. 2010;3(7):643-653.
14. Etich J, Koch M, Wagener R, Zaucke F, Fabri M, Brachvogel B. Gene expression profiling of the extracellular matrix signature in macrophages of different activation status: relevance for skin wound healing. *Int J Mol Sci*. 2019;20(20):5086.
15. Sokol CL, Luster AD. The chemokine system in innate immunity. *Cold Spring Harb Perspect Biol*. 2015;7(5):a016303.
16. Baum CL, Arpey CJ. Normal cutaneous wound healing: clinical correlation with cellular and molecular events. *Dermatol Surg*. 2005;31(6):674-686. discussion 86.
17. Rodrigues M, Kosaric N, Bonham CA, Gurtner GC. Wound healing: a cellular perspective. *Physiol Rev*. 2019;99(1):665-706.
18. Brubaker AL, Rendon JL, Ramirez L, Choudhry MA, Kovacs EJ. Reduced neutrophil chemotaxis and infiltration contributes to delayed resolution of cutaneous wound infection with advanced age. *J Immunol*. 2013;190(4):1746-1757.
19. James GA, Swogger E, Wolcott R, et al. Biofilms in chronic wounds. *Wound Repair Regen*. 2008;16(1):37-44.
20. Lazarus GS, Cooper DM, Knighton DR, Percoraro RE, Rodeheaver G, Robson MC. Definitions and guidelines for assessment of wounds and evaluation of healing. *Wound Repair Regen*. 1994;2(3):165-170.
21. Whittam AJ, Maan ZN, Duscher D, et al. Challenges and opportunities in drug delivery for wound healing. *Adv Wound Care*. 2016;5(2):79-88.
22. Miller KG, Tran PL, Haley CL, et al. Next science wound gel technology, a novel agent that inhibits biofilm development by gram-positive and gram-negative wound pathogens. *Antimicrob Agents Chemother*. 2014;58(6):3060-3072.
23. Fleming D, Chahin L, Rumbaugh K. Glycoside hydrolases degrade polymicrobial bacterial biofilms in wounds. *Antimicrob Agents Chemother*. 2017;61(2):e01998-e01916.
24. Hur W, Lee HY, Min HS, et al. Regeneration of full-thickness skin defects by differentiated adipose-derived stem cells into fibroblast-like cells by fibroblast-conditioned medium. *Stem Cell Res Ther*. 2017;8(1):92.
25. Lih E, Lee JS, Park KM, Park KD. Rapidly curable chitosan-PEG hydrogels as tissue adhesives for hemostasis and wound healing. *Acta Biomater*. 2012;8(9):3261-3269.
26. Zalipsky S. Functionalized poly(ethylene glycol) for preparation of biologically relevant conjugates. *Bioconjug Chem*. 1995;6(2):150-165.
27. Cardiff RD, Miller CH, Munn RJ. Manual hematoxylin and eosin staining of mouse tissue sections. *Cold Spring Harb Protoc*. 2014;2014(6):655-658.
28. Lin ZQ, Kondo T, Ishida Y, Takayasu T, Mukaida N. Essential involvement of IL-6 in the skin wound-healing process as evidenced by delayed wound healing in IL-6-deficient mice. *J Leukoc Biol*. 2003;73(6):713-721.

29. Swift ME, Kleinman HK, DiPietro LA. Impaired wound repair and delayed angiogenesis in aged mice. *Lab Invest*. 1999;79(12):1479-1487.
30. Cerqueira MT, da Silva LP, Santos TC, et al. Human skin cell fractions fail to self-organize within a gellan gum/hyaluronic acid matrix but positively influence early wound healing. *Tissue Eng Part A*. 2014;20(9–10):1369-1378.
31. Frontera-Acevedo K, Sakamoto K. Local pulmonary immune responses in domestic cats naturally infected with *Cytauxzoon felis*. *Vet Immunol Immunopathol*. 2015;163(1–2):1-7.
32. Lopes-Pacheco M, Ventura TG, de Oliveira HD, et al. Infusion of bone marrow mononuclear cells reduces lung fibrosis but not inflammation in the late stages of murine silicosis. *PLoS One*. 2014;9(10):e109982.
33. Choi SH, Kim AR, Nam JK, et al. Tumour-vasculature development via endothelial-to-mesenchymal transition after radiotherapy controls CD44v6(+) cancer cell and macrophage polarization. *Nat Commun*. 2018;9(1):5108.
34. Yan J, Tie G, Wang S, et al. Diabetes impairs wound healing by Dnmt1-dependent dysregulation of hematopoietic stem cells differentiation towards macrophages. *Nat Commun*. 2018;9(1):33.
35. Ortines RV, Liu H, Cheng LI, et al. Neutralizing alpha-toxin accelerates healing of *Staphylococcus aureus*-infected wounds in nondiabetic and diabetic mice. *Antimicrob Agents Chemother*. 2018;62(3):e02288-e02217.
36. Kruger NJ. The Bradford method for protein quantitation. *Methods Mol Biol*. 1994;32:9-15.
37. Batista MD, Ho EL, Kuebler PJ, et al. Skewed distribution of natural killer cells in psoriasis skin lesions. *Exp Dermatol*. 2013;22(1):64-66.
38. von Bubnoff D, Andres E, Hentges F, Bieber T, Michel T, Zimmer J. Natural killer cells in atopic and autoimmune diseases of the skin. *J Allergy Clin Immunol*. 2010;125(1):60-68.
39. Stevens WW, Kim TS, Pujanauski LM, Hao X, Braciale TJ. Detection and quantitation of eosinophils in the murine respiratory tract by flow cytometry. *J Immunol Methods*. 2007;327(1–2):63-74.
40. Clark RA. Fibrin and wound healing. *Ann N Y Acad Sci*. 2001;936:355-367.
41. Kim YS, Cho IH, Jeong MJ, et al. Therapeutic effect of total ginseng saponin on skin wound healing. *J Ginseng Res*. 2011;35(3):360-367.
42. Deer TR, Stewart CD. Wound healing. In: Deer TR, Pope JE, eds. *Atlas of Implantable Therapies for Pain Management*. New York, NY: Springer; 2016:89-92.
43. Werner S, Grose R. Regulation of wound healing by growth factors and cytokines. *Physiol Rev*. 2003;83(3):835-870.
44. Mrstik M, Kotseos K, Ma C, Chegini N. Increased expression of interferon-inducible protein-10 during surgically induced peritoneal injury. *Wound Repair Regen*. 2003;11(2):120-126.
45. Yates CC, Whaley D, Hooda S, Hebda PA, Bodnar RJ, Wells A. Delayed reepithelialization and basement membrane regeneration after wounding in mice lacking CXCR3. *Wound Repair Regen*. 2009;17(1):34-41.
46. Jin SG, Yousaf AM, Jang SW, et al. *In vivo* wound-healing effects of novel benzalkonium chloride-loaded hydrocolloid wound dressing. *Drug Dev Res*. 2015;76(3):157-165.
47. Broughton G 2nd, Janis JE, Attinger CE. Wound healing: an overview. *Plast Reconstr Surg*. 2006;117(7 Suppl):1e-S–32e-S.
48. Reinke JM, Sorg H. Wound repair and regeneration. *Eur Surg Res*. 2012;49(1):35-43.
49. Flanagan M. The physiology of wound healing. *J Wound Care*. 2000;9(6):299-300.
50. Khanna S, Biswas S, Shang Y, et al. Macrophage dysfunction impairs resolution of inflammation in the wounds of diabetic mice. *PLoS One*. 2010;5(3):e9539.
51. Mirza RE, Fang MM, Novak ML, et al. Macrophage PPARgamma and impaired wound healing in type 2 diabetes. *J Pathol*. 2015;236(4):433-444.
52. Nathan C. Neutrophils and immunity: challenges and opportunities. *Nat Rev Immunol*. 2006;6(3):173-182.
53. Dovi JV, He LK, DiPietro LA. Accelerated wound closure in neutrophil-depleted mice. *J Leukoc Biol*. 2003;73(4):448-455.
54. Low QE, Drugea IA, Duffner LA, et al. Wound healing in MIP-1alpha(−/−) and MCP-1(−/−) mice. *Am J Pathol*. 2001;159(2):457-463.
55. Nasruddin NY, Mukai K, HSE R, et al. Cold plasma on full-thickness cutaneous wound accelerates healing through promoting inflammation, re-epithelialization and wound contraction. *Clin Plasma Med*. 2014;2(1):28-35.
56. Nishiyama T, Kii I, Kashima TG, et al. Delayed re-epithelialization in periostin-deficient mice during cutaneous wound healing. *PLoS One*. 2011;6(4):e18410.
57. Pilcher BK, Wang M, Qin XJ, Parks WC, Senior RM, Welgus HG. Role of matrix metalloproteinases and their inhibition in cutaneous wound healing and allergic contact hypersensitivity. *Ann N Y Acad Sci*. 1999;878:12-24.
58. Wilgus TA, Roy S, McDaniel JC. Neutrophils and wound repair: positive actions and negative reactions. *Adv Wound Care*. 2013;2(7):379-388.
59. Tecchio C, Micheletti A, Cassatella MA. Neutrophil-derived cytokines: facts beyond expression. *Front Immunol*. 2014;5:508.
60. Parks WC. Matrix metalloproteinases in repair. *Wound Repair Regen*. 1999;7(6):423-432.
61. Rho CR, Park MY, Kang S. Effects of granulocyte-macrophage colony-stimulating (GM-CSF) factor on corneal epithelial cells in corneal wound healing model. *PLoS One*. 2015;10(9):e0138020.
62. Lim JY, Choi BH, Lee S, Jang YH, Choi JS, Kim YM. Regulation of wound healing by granulocyte-macrophage colony-stimulating factor after vocal fold injury. *PLoS One*. 2013;8(1):e54256.
63. Castrogiovanni P, Ventimiglia P, Imbesi R. Wound healing: experience with rHuGM-CSF. *Wounds*. 2010;22(10):256-260.
64. Capanema NSV, Mansur AAP, de Jesus AC, Carvalho SM, de Oliveira LC, Mansur HS. Superabsorbent crosslinked carboxymethyl cellulose-PEG hydrogels for potential wound dressing applications. *Int J Biol Macromol*. 2018;106:1218-1234.
65. Field FK, Kerstein MD. Overview of wound healing in a moist environment. *Am J Surg*. 1994;167(1A):2S-6S.
66. Hwang MR, Kim JO, Lee JH, et al. Gentamicin-loaded wound dressing with polyvinyl alcohol/dextran hydrogel: gel characterization and *in vivo* healing evaluation. *AAPS PharmSciTech*. 2010;11(3):1092-1103.
67. Thomason HA, Lovett JM, Spina CJ, Stephenson C, McBain AJ, Hardman MJ. Silver oxysalts promote cutaneous

wound healing independent of infection. *Wound Repair Regen*. 2018;26(2):144-152.

SUPPORTING INFORMATION

Additional supporting information may be found online in the Supporting Information section at the end of this article.

How to cite this article: Bounds K, Colmer-Hamood JA, Myntti M, Jeter RM, Hamood AN. The influence of a biofilm-dispersing wound gel on the wound healing process. *Int Wound J*. 2022;19(3):553-572. https://doi.org/10.1111/iwj.13653